

04 Apr 1995, 8:00 am - 9:00 am

Liquefaction-Induced Lateral Ground Displacement

T. Leslie Youd
Brigham Young University, Provo, Utah

Follow this and additional works at: <https://scholarsmine.mst.edu/icrageesd>



Part of the [Geotechnical Engineering Commons](#)

Recommended Citation

Youd, T. Leslie, "Liquefaction-Induced Lateral Ground Displacement" (1995). *International Conferences on Recent Advances in Geotechnical Earthquake Engineering and Soil Dynamics*. 3.
<https://scholarsmine.mst.edu/icrageesd/03icrageesd/session16/3>



This work is licensed under a [Creative Commons Attribution-Noncommercial-No Derivative Works 4.0 License](#).

This Article - Conference proceedings is brought to you for free and open access by Scholars' Mine. It has been accepted for inclusion in International Conferences on Recent Advances in Geotechnical Earthquake Engineering and Soil Dynamics by an authorized administrator of Scholars' Mine. This work is protected by U. S. Copyright Law. Unauthorized use including reproduction for redistribution requires the permission of the copyright holder. For more information, please contact scholarsmine@mst.edu.

Liquefaction-Induced Lateral Ground Displacement

Paper No. SOA6

(State of the Art Paper)

T. Leslie Youd

Professor of Civil Engineering, Brigham Young University, Provo, Utah

SYNOPSIS Ground displacements generated by liquefaction-induced lateral spread are a severe threat to engineered construction. During past earthquakes, lateral spread displacements have pulled apart or sheared shallow and deep foundations of buildings, severed pipelines and other structures and utilities that transect the ground displacement zone, buckled bridges or other structures constructed across the toe, and toppled retaining walls, bulkheads, etc. that lie in the path of the spreading ground. This paper presents a method for estimating probable free-field lateral displacements at sites susceptible to liquefaction. Free-field ground displacements are those that are not impeded by structural resistance, ground modification, or a natural boundary.

INTRODUCTION

Liquefaction of saturated granular soils and consequent ground deformation have been a major cause of damage to constructed works during past earthquakes. Loss of bearing strength, differential settlement, and horizontal displacement due to lateral spread are the major sources of damaging ground deformations beneath level- to gently-sloping sites, the types of terrain where most development has occurred. This paper provides procedures including equations, tables, and charts required to evaluate probable free-field lateral displacements. Free-field ground displacements are those that are not impeded by structural resistance, ground modification, or a natural boundary. Results using these procedures may be applied to assessment of ground-failure hazard to constructed or planned facilities, for initial lateral displacement design criteria (although structural impedance may prevent development of full free-field displacements), and for delineation of areas where liquefaction-induced earthquake damage might be expected. The methodologies and much of the text presented herein are taken from previous papers by Bartlett and Youd (1992) and Youd (1993).

MODES OF GROUND FAILURE

Liquefaction may lead to any one of three types of ground failure that produce lateral ground displacement: flow failure, lateral spread, and ground oscillation. The bounds between these failure types are transitional; which type of failure if any, depends on local site conditions.

Flow failures form on steep slopes (greater than 6%), are caused by a large reduction of soil strength (contractive soils), and are characterized by large displacements (commonly several meters or more) with substantial internal disruption of the mobilized soil mass (as depicted in Fig. 1). Fig. 2 shows a flow failure that developed in a highway fill at the western edge of Lake Merced in San Francisco during the 1957 Daly City earthquake.

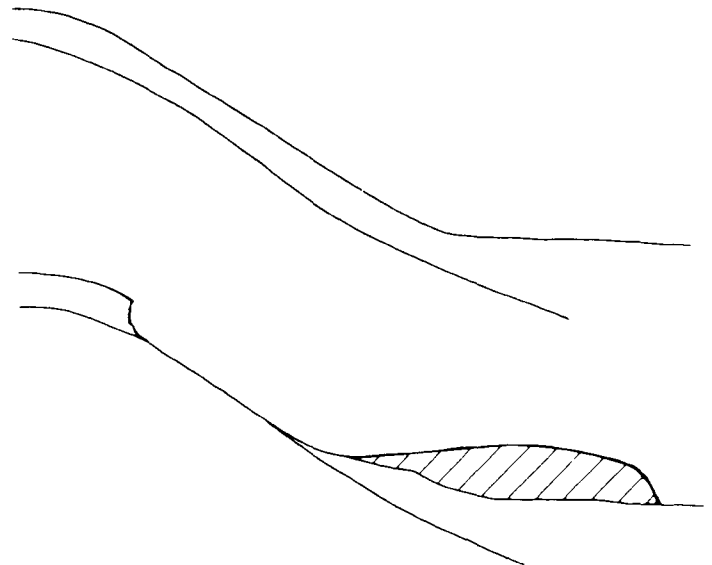


Fig. 1. Illustration of Flow Failure Caused by Liquefaction, Loss of Strength, and Massive Down-Slope Movement of Liquefied Soil (After Youd, 1993)

On the other end of the spectrum, **ground oscillation** generally occurs on flat ground with liquefaction at depth decoupling surface soil layers from the underlying unliquefied ground (Fig. 3). This decoupling allows rather large transient ground oscillations or ground waves to develop; the associated permanent displacements, however, are usually small and chaotic with respect to magnitude and direction. Observers of ground oscillation have described large-amplitude ground waves (up to several feet high) often accompanied by opening and closing of ground fissures, which in some instances have propelled ejected ground water to heights as great as several meters. For example, most of the chaotic ground movements which fractured and buckled pavements in the Marina District of San Francisco during the 1989 Loma Prieta earthquake were caused by ground oscillation (Fig. 4).



Fig. 2. Flow Failure Along Shoreline of Lake Merced, San Francisco, California, Triggered by Liquefaction During 1957 Daly City Earthquake (Photograph courtesy of U.S. Geological Survey)

Lateral spread lies between flow failure and ground oscillation on the ground failure spectrum and involves some components of both of these end members. Lateral spread is characterized primarily by horizontal displacement of surficial soil layers as a consequence of liquefaction of a subsurface granular deposit (Fig. 5). Displacement occurs in response to a combination of dynamic earthquake-generated inertial forces and static gravitational forces acting on soil layers within and above the liquefied zone. During failure, surface layers commonly break into large blocks which transiently shift back and forth and up and down in the form of ground waves (ground oscillation), but move progressively down slope. Lateral spreads generally move down gentle slopes (usually less than 6%) or slip toward a free face such as an incised river channel. Horizontal displacements may range from a few tenths of a meter to a few meters, but where ground conditions are particularly favorable or shaking is very intense or of long duration, displacements may be larger and may even approach a flow-failure condition. Fig. 6 shows the Marine Sciences Laboratory at Moss Landing, California, that was pulled apart by a lateral spread that migrated about 1.5 m down a mild slope during the 1989 Loma Prieta earthquake. A lateral spread with larger horizontal displacement (about 3.6 m) developed at that same site during the 1906 San Francisco earthquake.

The surface of a lateral spread is commonly disrupted by open fissures and scarps at the head of the failure, shear zones along the margins, and compressed or buckled soil at the toe. Ground fissures and small grabens also may develop within the interior of the mass. Differential vertical displacements may also occur as a consequence of down-slope movement, compaction of underlying granular sediment, or dynamic penetration or rise of discrete soil blocks. Lateral spreads commonly pull apart or shear foundations of buildings and other structures built on or across the head of the failure zone, sever pipelines and other structures and utilities that transect the lateral margins of the zone, and topple retaining walls or buckle pipelines, bridges or other structures constructed across the toe.

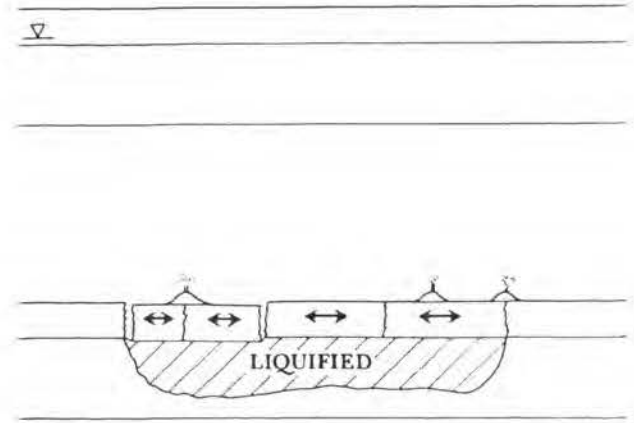


Fig. 3. Illustration of Ground Oscillation Caused by Liquefaction-Induced Decoupling of Surface Soil Layers Which Oscillate in Response to Earthquake Shaking (After Youd, 1993)



Fig. 4. Pavements and Curbs Disrupted by Ground Oscillation in the Marina District of San Francisco During 1989 Loma Prieta Earthquake (Photograph courtesy of Raymond B. Seed, University of California, Berkeley)

METHODS FOR ANALYZING LATERAL DISPLACEMENT

Several techniques have been proposed for estimating lateral ground displacements at liquefaction sites, including analytical models, physical models, and empirical correlations.

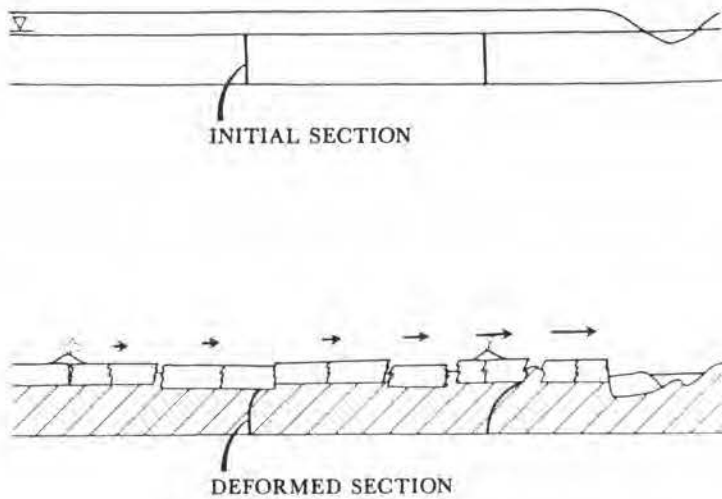


Fig. 5. Illustration of Lateral Spread Caused by Liquefaction-Induced Softening of Soils and Lateral Displacement of Surficial Soil Layers Down Slope or Toward a Free Face (After Youd, 1993)



Fig. 6. Building Pulled Apart by Liquefaction-Induced Lateral Spread During 1989 Loma Prieta, California, Earthquake (After Youd, 1993).

Finite Element Analyses

Non-linear finite element analyses have been proposed for evaluation of ground deformation at liquefaction sites, including the Princeton University effective stress model (Prevost, et al., 1986) and TARA-3FL (Finn and Yogendrakumar, 1989). These finite element analyses require constitutive stress-strain relationships and undrained steady state strength data, respectively. Because of inherent difficulties in sampling and testing to define these properties for field sites, applications of these procedures are usually limited to critical projects or to research.

Elastic Beam Analysis

Hamada et al. (1987), Towhata et al. (1991) and Yasuda et al. (1991) have used elastic models to predict lateral spread displacements from the 1964 Niigata and 1983 Nihonkai-Chubu earthquakes. The model proposed by Hamada et al. assumes that upon liquefaction, the frictional resistance between the liquefied subsurface soil and the non-liquefied surficial layer is zero. Therefore, they postulate that the non-liquefied surficial layer acts as a sloping elastic beam resisting on a frictionless soil layer. The surficial layer is then modeled as a 2-D surface that is allowed to strain under gravitational forces. The 2-D model proposed by Towhata et al. also treats the non-liquefied surficial layer as an elastic surface that resists the flow of the liquefied subsurface layer, but deformation of the soil profile is approximated by a sinusoidal curve with zero displacement at the base of the liquefied layer and a maximum displacement at the ground surface. Based on these assumptions, an analytical closed-form solution for ground displacement is obtained by minimizing the potential energy of the system.

The elastic model proposed by Yasuda et al. assumes that most of the permanent ground displacement in liquefied soils results from the pre-earthquake static shear stresses. In the first stage of the analysis, the shear stress distribution and pre-liquefaction strain is calculated by using the elastic modulus of the soil prior to liquefaction. Secondly, the analysis is repeated by keeping the pre-earthquake static stresses constant and using a reduced shear modulus for the liquefied soil. Ground displacement vectors are calculated by subtracting the results of the first analysis from the second.

Although some after-the-fact analyses using the elastic beam procedure have yielded results comparable to measured displacements, some poorly constrained assumptions, such as elastic moduli of the soil beam and shear moduli for the liquefied soil, create considerable uncertainty in the results. Also the assumption of a continuous elastic soil beam seems to be at variance with the fissured and fractured ground surface created by many lateral spreads.

Sliding-Block Analysis

Newmark (1965) introduced a rather simple mechanistic procedure for estimating the displacement of a rigid block resting on an inclined failure plane that is subjected to earthquake shaking. That model has been commonly modeled as a single-degree-of-freedom rigid plastic system. As Byrne et al. (1992) have noted, there are two concerns when applying Newmark's simple model to natural ground failures, such as lateral spreads: (1) the soil, particularly in liquefiable zones, is not adequately modeled as a rigid-plastic material; and (2) the single-degree-of-freedom model does not allow for a pattern of displacements to be computed. The latter deficiency is critical to lateral spreads near free faces, where displacements markedly decrease with distance from the free face. For this type of failure, a single-degree-of-freedom model is incapable of generating such a distribution of displacements. To overcome these obstacles, Byrne et al. (1992) have developed a more sophisticated model in which a deformational analysis incorporating pseudo-dynamic finite

element procedures allows for consideration of both inertia forces from the earthquake as well as softening of the liquefied soil. The method is an extension of Newmark's simple model to a flexible multi-degree-of-freedom system.

Application of the procedure by Byrne et al. (1992) requires evaluation of several model-specific soil properties and application of rather sophisticated computer programs, such as SOILSTRESS. This technique is still being developed; more testing and verification are needed before the procedure can be applied by non-specialists for routine engineering analyses. For analysis of critical structures, however, specialists are available to apply the procedure. The mechanistic technique has the advantage of most analytical models, in that possible remedial measures can be modeled and analyzed.

Physical Modeling

Physical modeling typically involves use of centrifuges or shaking tables to simulate prototype soils and seismic loading under well-defined boundary conditions. The soil used in such models is reconstituted to represent density and geometrical conditions. Because of difficulties in precisely modeling field conditions at natural sites, physical models have seldom been used in design. Physical models are valuable, however, for analyzing and understanding generalized soil behavior and for evaluating the validity of constitutive models.

Empirical Procedures

Because of the present difficulties in analytically or physically modeling soil conditions at most liquefiable sites, empirical procedures have become a standard procedure for evaluating liquefaction susceptibility and for estimating lateral spread displacement. Procedures developed by Bartlett and Youd (1992) for estimating displacements are given below. These empirical procedures have the advantage of using standard field tests, commonly determined soil textural properties, and easily obtained topographical information for estimating lateral displacement. Details on model development and case history site information utilized are given by Bartlett and Youd (1992).

For general engineering applications where a high degree of accuracy is not required, empirical analysis may be adequate and can be conservatively applied for basic engineering design. Where more accuracy is required, the empirical estimates may be improved by conducting more sophisticated finite element or mechanistic sliding-block analyses. For these more sophisticated analyses, more refined soil property data are required, such as constitutive stress-strain relations and steady state undrained or residual strengths. Because of the difficulty in precisely determining these more refined soil properties at natural field sites, estimates of displacements using the more sophisticated procedures may, in many instances, be no more accurate than the empirical estimates.

TABLE I. Earthquakes and Lateral Spread Sites Included in Case-History Database Compiled by Bartlett and Youd (1992)

<u>1906 San Francisco Earthquake ($M_w = 7.9$)</u>	
	Coyote Creek Bridge near Milpitas, California
	Mission Creek Zone in San Francisco, California
	Salinas River Bridge near Salinas, California
	South of Market Street Zone in San Francisco, California
<u>1964 Alaska Earthquake ($M_w = 9.2$)</u>	
	Bridges 141.1, 147.4, 147.5, 148.3, Matanuska River
	Bridges 63.0, 63.5, Portage Creek, Portage
	Highway Bridge 629, Placer River, (Ross et al., 1973)
	Highway Bridge 605A, Snow River, (Ross et al., 1973)
	Bridges 3.0, 3.2, 3.3, Resurrection River
<u>1964 Niigata, Japan, Earthquake ($M_w = 7.5$)</u>	
	Numerous lateral spreads in Niigata, Japan
<u>1971 San Fernando, California Earthquake ($M_w = 6.4$)</u>	
	Jensen Filtration Plant
	Juvenile Hall
<u>1979 Imperial Valley, California Earthquake ($M_w = 6.4$)</u>	
	Heber Road near El Centro, California
	River Park near Brawley, California
<u>1983 Borah Peak Idaho, Earthquake ($M_w = 6.9$)</u>	
	Whiskey Springs near Mackay, Idaho
	Pence Ranch near Mackay, Idaho
<u>1983 Nihonkai-Chubu Earthquake ($M_w = 7.7$)</u>	
	Lateral spreads in the Northern Sector of Noshiro, Japan
<u>1987 Superstition Hills Earthquake ($M_w = 6.6$)</u>	
	Wildlife Instrument Array, Brawley, CA

DEVELOPMENT OF EMPIRICAL EQUATIONS

Bartlett and Youd (1992) collected lateral spread case history data from eight earthquakes and numerous lateral spreads. The earthquakes and principle localities of spreading are listed in Table I. Six of the earthquakes are from the western U.S. and the other two are from Japan. The lateral spread data from the Japanese earthquakes are from a narrow range of seismic conditions, magnitude 7.5 and 7.7 earthquakes at source distances of 21 to 30 km. The six U.S. earthquakes span a wider range of magnitudes (6.4 to 9.2) and greater range of source distances (up to 90 km), but all come from the western U.S., which is characterized by relatively high ground motion attenuation with distance from the seismic source. Also, most of the lateral spread areas are underlain by stiff soils (mostly deep profiles of cohesionless sands and/or overconsolidated silts and clays). Thus, the observational data are primarily from stiff sites in regions of relatively high ground motion attenuation.

From published case-histories of lateral spreads, Bartlett and Youd compiled a database of 448 horizontal displacement vectors and 270 associated nearby bore-hole logs. To increase the database for distant sites, they added information for 19 sites near the maximum distance bound for observed liquefaction effects (Ambraseys, 1988). Those distant sites are primarily from the western U.S. Effects at those distant sites typically consisted of a few small sand boils and, in some instances, a few small fissures. Lateral displacement and soil-property information were not reported for those distant sites. To provide reasonable estimates for the regression analysis, Bartlett and Youd assigned uniform displacements of 0.05 m to each of the distant sites, and uniform soil profiles consisting of the average thicknesses and soil properties of sediments beneath the lateral spreads in the database. From these compiled data, Bartlett and Youd applied the technique of stepwise multiple linear regression (MLR) to first define the factors that most influence ground displacement, and then to construct a regression model incorporating those factors.

Several possible seismic, geometric, and soil factors were considered in the regression analyses. Although seismic factors, such as peak acceleration, a_{max} , and duration of strong shaking, t_{ss} , should be fundamental parameters controlling displacement, the regression yielded better results (higher correlation coefficients) when magnitude, M , and horizontal distance from the seismic source, R , were used as seismic parameters. One reason M and R performed better is that those parameters could be directly measured, whereas a lack of instrumental records at lateral spread sites necessitated the estimation of a_{max} and t_{ss} from M and R . Therefore, the regression model is expressed in terms of M and R .

To incorporate the influence of geometric factors, two statistically independent models are required: a free-face model for areas near steep banks, and a ground-slope model for areas with gently sloping terrain. Several soil factors were tested in the models; those that were statistically significant are incorporated into the following equations.

For free-face conditions:

$$\begin{aligned} \text{LOG } D_H = & -16.3658 + 1.1782 M - 0.9275 \text{ LOG } R \\ & - 0.0133 R + 0.6572 \text{ LOG } W + 0.3483 \text{ LOG } T_{15} \\ & + 4.5270 \text{ LOG } (100 - F_{15}) - 0.9224 D50_{15} \end{aligned} \quad (1a)$$

For ground slope conditions:

$$\begin{aligned} \text{LOG } D_H = & -15.7870 + 1.1782 M - 0.9275 \text{ LOG } R \\ & - 0.0133 R + 0.4293 \text{ LOG } S + 0.3483 \text{ LOG } T_{15} \\ & + 4.5270 \text{ LOG } (100 - F_{15}) - 0.9224 D50_{15} \end{aligned} \quad (1b)$$

Where:

- D_H = Estimated lateral ground displacement, in m.
- $D50_{15}$ = Average mean-grain size in granular layers included in T_{15} , in mm.
- F_{15} = Average fines content (fraction of sediment sample passing a No. 200 sieve) for granular layers included in T_{15} , in percent.

TABLE II. Ranges of Input Values Listed by Bartlett and Youd (1992) for Which Predicted Results Are Verified by-Case-History Observations

Input Factor	Range of Values in Case History Database
Magnitude	$6.0 < M < 8.0$
Free-Face Ratio	$1.0\% < W < 20\%$
Ground Slope	$0.1\% < S < 6\%$
Thickness of Loose Layer	$0.3 \text{ m} < T_{15} < 12 \text{ m}$
Fines Content	$0\% < F_{15} < 50\%$
Mean Grain Size	$0.1 \text{ mm} < D50_{15} < 1 \text{ mm}$
Depth to Bottom of Section	Depth to Bottom of Liquefied Zone $< 15 \text{ m}$

- M = Earthquake magnitude (moment magnitude).
- R = Horizontal distance from the seismic energy source, in km.
- S = Ground slope, in percent.
- T_{15} = Cumulative thickness of saturated granular layers with corrected blow count, $(N_1)_{60}$ less than 15, in m
- W = Ratio of the height (H) of the free face to the distance (L) from the base of the free face to the point in question, in percent (Fig. 7).

The regression coefficient, r^2 , for these models is 83%. The allowable ranges of the independent variables (imputed values) are listed in Table II. Because there are few measured displacements greater than 10 m in the data set, Equation 1 may not reliably predict values larger than that amount. Extrapolation to values beyond the limits listed in Table 2 yields uncertain predictions. The limits of each independent variable are further discussed in the following section.

To show the predictive performance of the above equations, Bartlett and Youd plotted predicted displacements against measured displacements recorded in the observational database (Fig. 8). The solid diagonal line on the figure represents perfect prediction, i.e., predicted displacement equals measured displacement. The lower dashed line represents 100% over prediction, and the dashed upper line represents 50% under prediction. Approximately 90% of the data plot between these two dashed bounds. This grouping indicates that predicted displacements are generally valid within a factor of 2 and that doubling of the predicted displacement provides a displacement estimate with a high probability of not being exceeded.

Only a few points plot above the upper dashed line in Fig. 8. These points represent lateral spreads where the measured displacement exceeded twice the predicted displacement. Poor quality of subsurface information may be a reason for several of these severe under-predictions of displacements at Japanese sites. The one severe under-prediction for a U.S. site is from a lateral spread that severely damaged the San Fernando Valley Juvenile Hall during the 1971 San Fernando earthquake. An examination of subsurface data from that site revealed that the sediments had some of the highest fines contents in the data set. Those sediments were also locally variable, and probably layered. For the regression analysis, the sediments incorporated in layer T_{15} were characterized by a single average fines content of 59% and single mean grain size of 0.06 mm. If a continuous sub-layer of cleaner and coarser sediments passes beneath the site, which appears likely but can not be confirmed from the sparse available data, then a separate analysis of that layer could lead to greater predicted displacement and a smaller degree of over-prediction. In addition to the fines content, other factors for this site are at the extremes of the data set. For example, this site is within the crustal uplift zone for the 1971 earthquake; thus the value of R is small and somewhat uncertain. The averaged textural values characterized by an F_{15} of 59% and a D_{50} of 0.06 mm are both beyond the suggested input limits listed in Table II. Thus, the extrapolation of the model to these conditions contains considerable uncertainty and may be the cause of the severe under-prediction.

The over-prediction of displacement at a number of sites is less problematic because over-prediction may lead to over-design, but not generally to an unsafe design. Most of the over-predicted displacements are for U.S. sites where measured displacements were less than 1 m. These measurements were generally taken near the margins of lateral spreads or on narrow, and in some instances sinuous, lateral spreads, where lateral boundary constraints may have hampered displacement. Thus, Equation 1 may significantly over-predict displacements near margins of spreads and at other localities where boundary effects retard lateral movement.

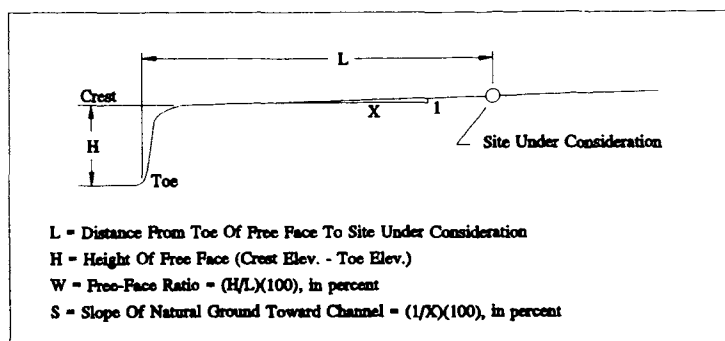


Fig. 7. Diagram Defining Ground Slope, S , and Free-Face Ratio, W (After Bartlett and Youd, 1992)

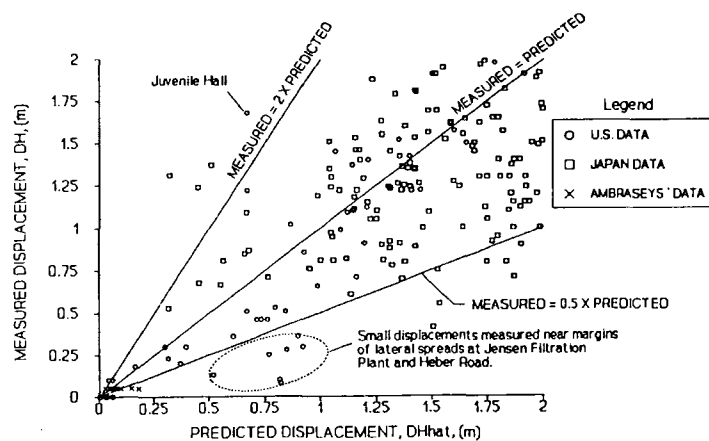


Fig. 8. Measured Versus Predicted Displacements Using Equations 1a and 1b and Data From Past Lateral Spreads (After Bartlett and Youd, 1992)

Equation 1 is generally valid for stiff-soil sites in the Western U.S. or within 30 km of the seismic source in Japan, i.e., the localities from which the case-history data were collected. For these regions and conditions, Equation 1 should be used directly to estimate displacement. For other regions of the world, such as the eastern U.S. where ground motions attenuate more slowly with distance, or for other site conditions, such as liquefiable deposits overlying soft clay layers, where ground motions may be strongly amplified, a correction must be applied to Equation 1 to account for these different conditions.

A preferred method to correct Equation 1 would be to regress the model in terms of more flexible parameters, such as M and a_{max} . However, because a_{max} have been measured at only a few lateral spread sites, a direct regression in terms of M and a_{max} is not possible. Attempts by Bartlett and Youd (1992) to develop a regression model based on estimated a_{max} yielded unsatisfactory results (poor correlation coefficients and poor predictions for case-history sites).

As an interim correction measure, until more case history data is assembled which will allow better correlation, Bartlett and Youd (1992) propose the following procedure for estimating displacements for sites with greater peak accelerations than would occur on stiff sites in the western U.S. In this procedure, a corrected distance term, R_{eq} , is applied in Equation 1 in place of the measured distance R . That factor is determined from the curves plotted in Fig. 9. Fig. 9 shows calculated distances, R_{eq} , at which a given a_{max} occurs for a given earthquake magnitude, M_w , for stiff soil sites in the western U.S. Those R_{eq} were calculated using attenuation equations proposed by Idriss (in press) and soil amplification factors published by Seed et al. (1994).

Specifically, the R_{eq} plotted in Fig. 9 were calculated as follows: the peak-acceleration attenuation criteria developed by Idriss were used to calculate peak-acceleration for rock-outcrop sites for a matrix of distances and earthquake

magnitudes. A style factor of 0.5 (oblique faulting) was assumed in the attenuation equations. To adjust the rock-outcrop values to stiff site conditions, Bartlett and Youd multiplied the acceleration values calculated for rock sites by a preliminary correction factor estimated from the peak-acceleration amplification curve published by Idriss (1990). More recently, however, Seed et al. (1994) have developed a more rigorous set of amplification curves for a variety of site stiffness conditions (Fig. 10); those curves are used herein. In Fig. 10, the curve labeled " C_4+D+E " is approximately the same as the curve suggested by Idriss (1990) for soft soil sites. The curve labeled " $B+C_1$ to C_3 " is a curve Seed et al. (1994) developed for stiff soil sites. Each of the rock-outcrop accelerations estimated from the Idriss criteria were then multiplied by an amplification factor for stiff sites taken directly from curve " $B+C_1$ to C_3 " in Fig. 10. The curves in Fig. 9 were then compiled by plotting distances at which a given a_{max} occurs on stiff soils for a variety of earthquake magnitudes. The compiled distances were then contoured to give the R_{eq} curves plotted in the figure.

The procedure for using the curves in Fig. 9 to correct Equation 1 for non-stiff and non-western U.S. sites is as follows. A design earthquake magnitude, M_w , and peak acceleration, a_{max} , are determined for the candidate site. That magnitude and acceleration are then plotted on Fig. 9 and an equivalent source distance, R_{eq} , is interpolated. That R_{eq} is then entered into Equation 1 in place of the actual source distance to calculate the estimated displacement. For example, during the 1989 Loma Prieta, California earthquake ($M_w = 6.9$), liquefaction and minor lateral spreading with up to 0.3 m of displacement were reported on Treasure Island at a distance of about 80 km from the seismic energy source. Application of that distance in Equation 1 along with appropriate soil and site properties indicates that lateral displacement should not have occurred. Considerable ground motion amplification occurred at Treasure Island, however, due to amplification of ground motions through the soft hydraulic fill and San Francisco Bay mud deposits underlying the island. Measured a_{max} on the Island was 0.16 g, whereas maximum bedrock accelerations measured in the area, including a record from Yerba Buena Island just a few thousand feet from Treasure Island, were roughly 0.07 g, and accelerations measured on stiff soil sites in the area were about 0.1 g. Thus, the measured acceleration on Treasure Island was more than twice the bedrock acceleration, and much larger than those on stiff soil sites. Plotting of a magnitude of 6.9 and an a_{max} of 0.16 on Fig. 9 yields an R_{eq} of about 40 km (compared to the actual source distance of 80 km). Entering an R_{eq} of 40 km into Equation 1a along with appropriate site and soil properties yields a predicted lateral displacement of a few tenths of a meter. These displacements roughly match the displacements observed following the earthquake.

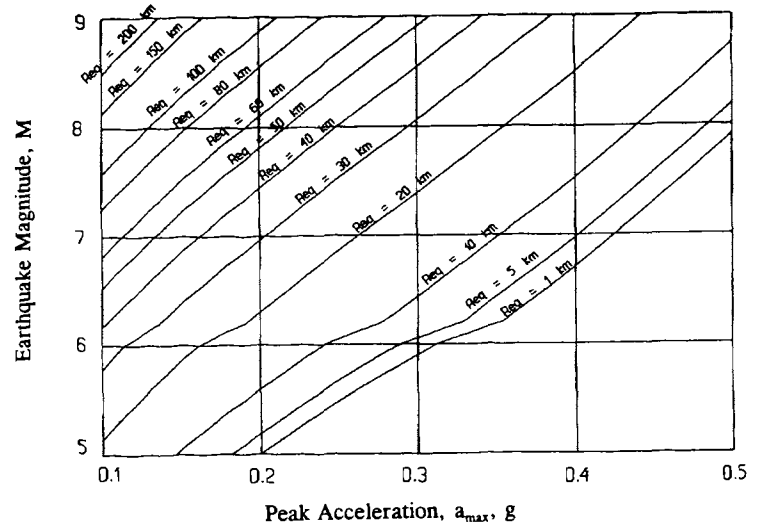


Fig. 9. Graph for Determining Equivalent Source Distance, R_{eq} , From Magnitude and Estimated a_{max} (After Bartlett and Youd, 1992)

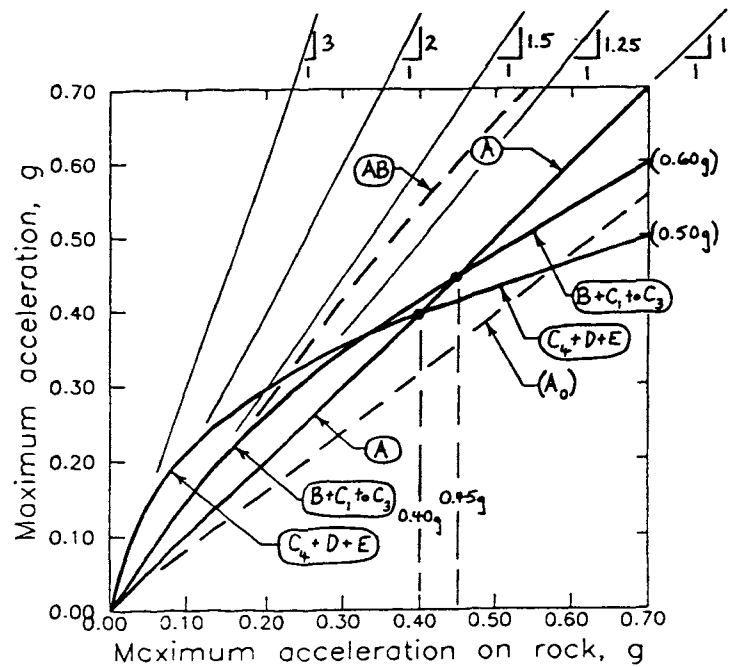


Fig. 10. Approximate Curves For Estimating a_{max} For Sites With Various Soil Stiffnesses (After Seed and others, 1994)

APPLICATION OF EQUATIONS

The general steps for calculating lateral spread displacement are diagrammed on the flow chart in Fig. 11. These steps define a procedure for estimating free-field displacements for engineering analyses. Also listed on the chart are the recommended ranges of input values from Table II, for which predicted displacements have been verified by comparison with the case-history data. Extrapolation beyond those limits, while sometimes allowable, will lead to greater uncertainty in predicted displacements.

Step 1

The first step in estimating lateral ground displacement is to perform a standard analysis of liquefaction susceptibility for the site in question. The "simplified procedure" developed by Seed and his colleagues (Seed et al., 1985) may be used for this analysis. If the susceptibility evaluation indicates a factor of safety against liquefaction greater than 1.2 for all granular layers, then lateral displacement should not occur and further analyses of liquefaction and lateral ground displacement are unnecessary. The use of a safety factor of 1.2 rather than 1.0 adds a margin of safety to account for uncertainty in the liquefaction analysis.

Step 2

If the analysis in Step 1 indicates a potential for liquefaction at the site, then the evaluation proceeds as follows: $(N_1)_{60}$ values are calculated at incremental depths in each of the saturated granular layers beneath the site. Sufficient SPT or CPT tests should be conducted to adequately characterize each granular layer in the soil profile. Sufficient borings or soundings should be made to adequately define the extent of potentially liquefiable soil layers beneath the area, which may extend well beyond the boundaries of the specific site in question.

The procedure used to calculate $(N_1)_{60}$ is the same as that specified for assessment of liquefaction susceptibility. If $(N_1)_{60}$ values equal to or smaller than 15 are not present in granular sediments, then lateral displacements would be small for earthquakes with magnitudes less than 8, and no further analysis is required.

Step 3

If liquefiable sediments, characterized by $(N_1)_{60}$ values less than 15, lie beneath the site, then the analysis proceeds to an evaluation of ground displacement using Equation 1. To apply this analysis, the following seismic, geometric and soil properties are needed.

(1) **Earthquake Magnitude, M .** The same earthquake magnitude, M , should be used in the analysis of lateral displacement as was used in the analysis of liquefaction susceptibility. Preferably moment magnitude, M_w , should be used in these analyses, but for magnitudes less than 7.5, estimates of either M_s or M_L may be substituted for M_w . Most of the case history data compiled by Bartlett and Youd (1992) are from earthquakes with magnitudes between 6 and 8. Extrapolation of Equation 1 to magnitudes beyond that range will increase uncertainty in the predicted values. However, because predicted displacement decreases markedly with magnitude, extrapolation to magnitudes smaller than 6 will usually yield small displacements, which, with conservative allowance for the greater uncertainty, are generally usable for engineering analyses. Extrapolation to

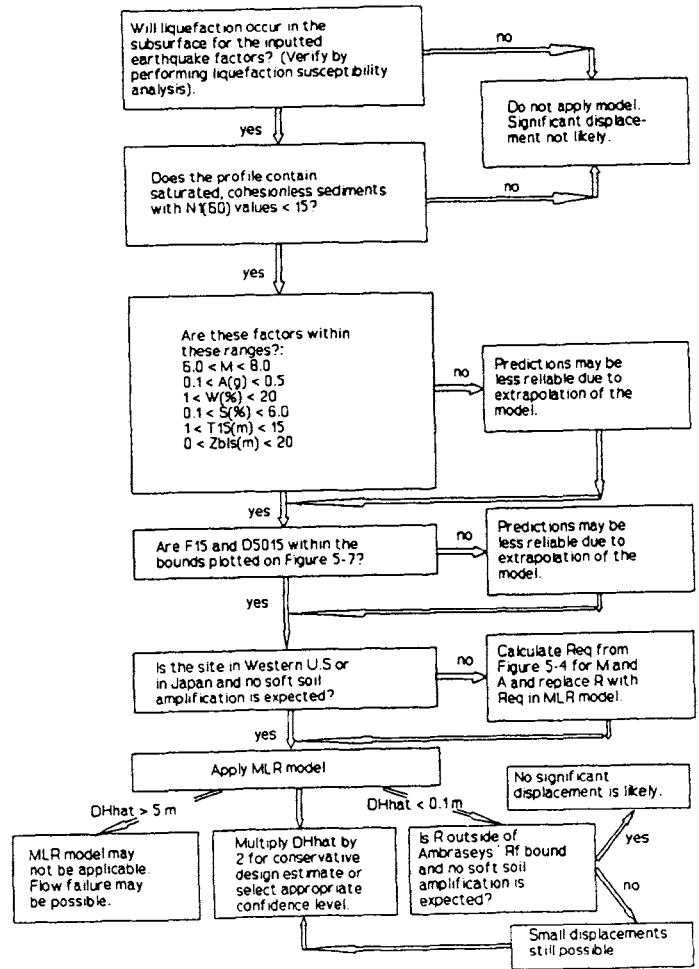


Fig. 11. Flow Chart For Application of Equation 1 (After Bartlett and Youd, 1992)

earthquakes with magnitudes greater than 8 appears to give reasonable predictions of displacement. For example, the predicted displacements agree well with measurements at a few non-gravelly sites where displacements were surveyed following the 1964 Alaska earthquake ($M_w = 9.2$). The amount of data available from these larger events, however, is too meager to provide adequate statistical constraint on the regression analysis. Thus, extrapolation to magnitudes larger than 8 introduces additional uncertainty in the predicted results.

(2) **Seismic Source Distance, R .** The seismic source distance, R , is defined as the horizontal distance in kilometers from the site in question to the nearest point on a surface projection of the seismic source zone. For earthquakes with magnitudes less than 6, the epicentral distances may be an adequate estimate for R . Earthquakes with magnitudes greater than 6, however, are generally associated with a large fault rupture zone that is not adequately characterized by single point such as an epicenter, and epicentral distances should not be used. Source zones for strike-slip and normal faults are commonly delineated by

a band incorporating surface ruptures produced by recent (Holocene) faulting events. For these types of faults, which are commonly in the western US, source distances may be measured directly from the edge of the surface rupture zone to the site in question. For reverse faults, shallow-angle thrusts, and subduction-zone earthquakes, the associated zone of tectonic crustal uplift generally delineates the surface projection of the seismic source zone. For these types of faults, the source distance is generally measured from the nearest point on the anticipated tectonic uplift zone to the site in question.

For poorly defined earthquake sources or diffuse seismic zones, such as occur in the eastern U.S., the minimal source distances noted in the next section should be used for sites within delineated seismic zones. Distances to the edge of the zone should be used for sites outside of the delineated zones.

Because few data from lateral spreads very near the source (small values of R) are included in the database developed by Bartlett and Youd (1992), extrapolation of Equation 1 to small R -distances yields unreliable estimates of lateral displacement. To reduce the possibility of such extrapolation error, Bartlett and Youd suggest a set of lower-limit values for R (Table III) which should not be subverted in applying Equation 1. Extrapolation below those limits will give uncertain predictions of lateral displacement.

(3) Peak Acceleration, a_{max} . Equation 1 is valid primarily for stiff soil sites in the western U.S. For soft soil sites, where ground motion amplification may occur, or for eastern U.S. sites, where strong ground motions propagate to greater distances than in the west, a correction is required to account for those greater ground motions. That correction is accomplished by correcting the distance term, R , used in equation 1 to R_{eq} by the following procedure. For non-western U.S. sites or for sites with high ground-motion amplification characteristics, R_{eq} is determined from the design seismic factors of magnitude, M , and a_{max} estimated for site in question. The values for these seismic factors would usually be the same as those used in the liquefaction analysis. The required a_{max} is plotted against magnitude on Fig. 9, and the equivalent source distance, R_{eq} is interpolated from the R_{eq} curves. The derived R_{eq} is then used in Equation 1. This procedure is only valid for a_{max} less than about 0.4 g and earthquake magnitudes less than 8. Extrapolation beyond these values will lead to less certain predictions. Also, mean values of predicted a_{max} should be used in the analysis, rather than mean plus one standard deviation or some other more conservative value. A greater degree of conservatism or probability of exceedance can then be applied, if required, to predicted displacement values.

As an example, assume that an eastern U.S. earthquake of magnitude 7.5 is estimated to produce a mean a_{max} of about 0.20 g at a source distance of 90 km. By plotting an a_{max} of

TABLE III. Minimum Values of R for Use in Equations 1 and 2. (After Bartlett and Youd, 1992)

Magnitude M_w	Minimum Value of R km
6.0	0.5
6.5	1
7.0	5
7.5	10
8.0	20-30

0.20 g against a magnitude, M , of 7.5 on Fig. 9, an R_{eq} of about 42 km is determined. The 42-km value is then applied as the R -value in equation 1.

(4) Free-Face Ratio, W . The definition of free-face ratio and the measurements required to calculate this parameter are illustrated in Fig. 7. The height of the free face, H , is defined as the vertical distance between the base and the crest of the free-face. That height is commonly determined by subtracting the elevation at the base, such as at the base of a river bank or at the toe of a fill, from the elevation at the top of the slope, such as at the top of a river bank or crest of an embankment. The distance, L , is measured from the base or toe of the free face to the locality in question. The free-face ratio, W , is then calculated from the relationship:

$$W = (H/L)(100), \text{ in percent} \quad (2)$$

Most values of W in the data set compiled by Bartlett and Youd (1992) lie between 1% and 20%. Extrapolation to values beyond that range will lead to great uncertainty in predicted displacements. For free-face ratios greater than 20%, gravitational forces may be sufficiently large for liquefaction to trigger either a flow failure or a rotational slump. In either instance, displacements may be larger than those predicted by Equation 1a.

Free-face ratios less than 1% generally lead to small predicted displacements which may be used with conservatism for flat ground conditions. However, in areas of sloping terrain, calculations should also be made using Equation 1b for sloping ground conditions. The larger of the two calculated displacements should be utilized for design or other applications.

(5) Slope, S . The ground slope, S , corresponds to the standard engineering definition of slope, that is the rise of elevation over the horizontal run of the slope (Fig. 7). For a unit rise of elevation, say 1 m over a horizontal distance of X m, the slope is:

$$S = (1/X)(100), \text{ in percent} \quad (3)$$

Where both sloping ground and a free face may affect lateral ground displacement at a site, calculations should be made using both Equations 1a and 1b. The larger of these two predictions should be used to estimate the ground displacement.

Ground slopes in the database compiled by Bartlett and Youd (1992) range from 0.1% to about 6%. Extrapolation beyond this range will lead to uncertain predictions. For slopes less than 0.1%, chaotic displacements due to ground oscillation are likely to exceed those from lateral spread. Thus, Equation 1 may give uncertain estimates of lateral displacement for flat ground conditions. Ground slopes that exceed 6% may be subject to flow failure and consequent large displacements. Equation 1 is not valid for estimating flow-failure displacements.

(6) **Thickness of loose granular sediment, T_{15} .** The thickness of loose granular layers in the sediment cross section is an important factor controlling amount of lateral ground displacement at liquefaction sites. Bartlett and Youd (1992) define that parameter as the thickness of granular layers in a sediment profile characterized by an $(N_1)_{60}$ equal to or less than 15. Fig. 12 illustrates the determination of T_{15} . That figure shows $(N_1)_{60}$ plotted against depth along with a dashed line marking an $(N_1)_{60}$ of 15. A stippled band paralleling the dashed line indicates depths where $(N_1)_{60}$ is less than 15. There are several possible choices for defining T_{15} for this illustration:

(a) One could sum the intervals marked by the stippled band shown on the fig. 12. That interpretation yields two segments of sediment characterized by $(N_1)_{60}$ less than 15, a segment between depths of 5 ft and 11 ft, and a second segment between depths of 14 ft and 20 ft. The total length of these two segments is 12 ft. That length, when applied in Equation 1, would yield smaller estimated displacements than the choices noted below. That smaller estimate may underestimate the displacement that is most likely to occur. Thus, this option is unsafe.

(b) Because only one $(N_1)_{60}$ value exceeds 15 in the depth interval between 5 ft and 20 ft, that value should be disregarded for conservative design in determining T_{15} . That $(N_1)_{60}$ may have been anomalous (the penetrometer may have hit a stone or other obstruction) or the reading may have been erroneous. Even if the $(N_1)_{60}$ is correct, the factor of safety against liquefaction is only slightly greater than unity, indicating that the soil at the depth in question could soften and participate to some degree in ground deformation. If two or more consecutive tests yield $(N_1)_{60}$ greater than 15, then a denser layer is more certain, and the intervening depth segment may be excluded from T_{15} . Finally, because a larger displacement is calculated by including the questionable segment than omitting it, that segment should be included in T_{15} to be conservatively safe. Using this option,

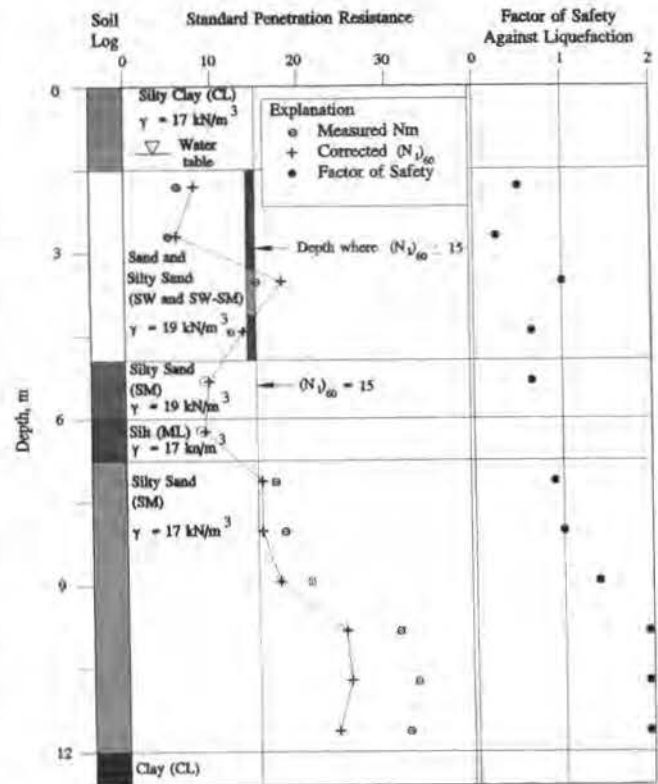


Fig. 12. Hypothetical Soil Profile for Illustrative Radar Tower Site (After Youd, 1993)

thickness T_{15} is defined as 15 ft, which includes all the sediment between depths of 5 and 20 ft.

(c) Two layers with distinctly different textures are incorporated in T_{15} as defined above, a sand to silty sand between depths of 1.5 and 5.1 m, and a silty sand between depths of 5.1 m and 6.0 m. Combination of these two layers, which requires averaged soil properties for the analysis, leads to smaller estimated displacements than when the layers are considered separately. Thus for conservative design, the two layers should be defined separately. Analyses using Equation 1 should be made for each layer and the predicted displacements from the separate analyses summed to provide the final estimate of displacement.

An examination of the soil stratigraphy illustrated in Fig. 12 suggests that a further definition of layers might be considered to separate the sand (SW), between 1.5 m and 3.3 m, from the sand to silty sand-(SW-SM), between 3.3 m and 5.1 m. Because the textural differences between these layers are not great, the latter separation would make only a small difference (but a slight increase) in the estimated displacement. Thus, whether or not to make this additional separation is a matter of engineering judgement. However, for this method of analysis, sub-layers should not be defined unless there are significant textural differences between the sub-layers.

For soil layers composed of thinly laminated materials (sub-layers less than 0.3 m thick) or thinly interbedded sediments, T_{15} should be defined as the total thickness of the layer rather than the thinner sub-layers, and the soil properties (F_{15} and $D50_{15}$) should be averaged over the entire layer.

One additional aspect of the calculation of T_{15} is illustrated by the soil profile depicted in Fig. 12. There is a marginally liquefiable layer between depths of 6.9 m and 9.6 m, with factors of safety against liquefaction ranging from 0.92 to 1.42. $(N_1)_{60}$'s over that same interval range from 15.9 to 17.7. Because these $(N_1)_{60}$'s exceed 15, this layer need not be included in T_{15} .

Although not shown on the soil profile illustrated in Fig. 12, some granular soil layers in a soil profile may be characterized by an $(N_1)_{60}$ less than 15, and yet have a factor of safety against liquefaction greater than 1.2. This condition commonly occurs at sites subjected to small-magnitude earthquakes or low levels of seismic shaking. Such non-liquefiable layers should not be included in T_{15} .

The thicknesses, T_{15} , in the case history data compiled by Bartlett and Youd range from 0.3 m to 15 m. Extrapolation beyond that range will lead to uncertain predictions. Extrapolation to thickness less than 0.3 m, however, should generally yield relatively small estimated displacements. Conservative assessment of displacement based on these predictions may be used for engineering analysis.

Liquefiable granular layers with thicknesses greater than 15 m are unusual in natural sediments. Extrapolation of Equation 1 to these unusual thicknesses will add uncertainty to the predicted displacements. Because it is unlikely that the entire thickness of such a layer would participate equally in producing ground displacement, the predicted displacements are likely to be greater than actual displacements. Such predictions may be used with engineering judgement for estimating conservative displacements for routine design applications.

(7) Average Fines Content, F_{15} . The regression analysis of Bartlett and Youd (1992), indicates that fines content, the percentage of material in a soil passing the No. 200 sieve (finer than 0.074 mm), is a major factor affecting the lateral ground displacement. Equation 1 indicates that the greater the fines content, the smaller the displacement of lateral spreads (all other factors remaining equal). To characterize the fines content of a liquefiable soil, Bartlett and Youd introduced the term F_{15} which is defined as the average fines content of materials included in a layer T_{15} . For example, referring to Fig. 12, the F_{15} for sand to silty-sand layer between depths of 1.5 m and 5.1 m would be the average of the fines contents from tests on four individual samples taken from that layer as listed in Table IV, or:

$$F_{15} = (3\% + 5\% + 10\% + 8\%)/4 = 6.5\%$$

TABLE IV. Data and Results from Calculations of Liquefaction Susceptibility For A Magnitude 6.5 Earthquake Generating an 0.30 g Peak Acceleration Shaking The Soil Profile Shown in Figure 12 (After Youd, 1993)

Depth m	Soil Description	N_m blows	$(N_1)_{60}$ blows	Fines %	Clay %	D_{50} mm	Factor of Safety
1	Silty clay (CL)	NA		87	43		NA
2	Sand (SW)	6	8.5 ?	3	0	0.43	0.50
3	Sand (SW)	5	6.2 ?	5	0	0.51	0.26
4	Sand with silt (SW-SM)	15	18.6	10	0	0.31	1.02
5	Sand with silt (SW-SM)	12	13.6	8	0	0.37	0.63
6	Silty sand (SM)	9	9.4	43	2	0.11	0.66
7	Silt (ML)	9	8.8	88	13	0.03	NA
8	Silty sand (SM)	17	15.9	21	0	0.22	0.92
9	Silty sand (SM)	18	15.9	30	1	0.20	1.00
10	Silty sand (SM)	21	17.7	37	1	0.18	1.42
11	Silty sand (SM)	31	25.1	35	0	0.25	>2
12	Silty sand (SM)	33	25.6	28	0	0.23	>2
13	Silty sand (SM)	32	24.0	18	0	0.30	>2
14	Clay (ML)						

If that layer were to be divided into two sub-layers (from 1.5 m to 3.3 m, and 3.3 m to 5.1 m) then the F_{15} for the upper layer would be 4%, and the F_{15} for the lower layer would be 9%.

As noted in the previous section, because of the large difference in fines content for this illustration between the silty sand (SM) compared to the overlying cleaner sands, a separate T_{15} layer should be defined for the silty sand (5.1 m to 6.0 m). Because only one sample was taken from that layer, the average fines content, F_{15} , for that layer is estimated as 43%.

Most of the F_{15} estimates in the data set compiled by Bartlett and Youd (1992) are between 0 and 50%. Extrapolation to fines contents greater than 50% leads to uncertain predictions.

(8) Average Mean-Grain Size, $D50_{15}$. The regression analysis by Bartlett and Youd (1992) shows that lateral ground displacement generally decreases with increased coarseness of the liquefiable material. They characterized that coarseness by the parameter, $D50_{15}$, which is the average mean-grain size of materials included in layer T_{15} . For example, for the sand to silty sand layer between depths of 1.5 m and 5.1 m as illustrated on Fig. 12, the average mean grain size is:

$$D50_{15} = (0.43 \text{ mm} + 0.51 \text{ mm} + 0.31 \text{ mm} + 0.37 \text{ mm})/4 = 0.405 \text{ mm}$$

For the underlying silty sand layer, $D50_{15}$ is approximated by the single measured mean-grain size of 0.11 mm.

The mean-grain sizes, $D50_{15}$, for which Equation 1 is valid, range from 0.1 mm to 1.0 mm. Data in the case histories do not support extrapolation of $D50_{15}$ for granular soils to values beyond this range. Extrapolation to finer grained soils adds uncertainty to the predicted values; these predicted displacements, however, are generally small and may be used with caution for ordinary design. If the finer-grained soils are collapsible or have sensitivities greater than about 1.5, displacements may be large and Equation 1 should not be applied. Extrapolation to mean grain sizes greater than 1 mm adds great uncertainty to the predicted displacements. For example, comparison of measured and predicted displacements from sites where liquefaction of coarse grained materials has occurred in past earthquakes, yields estimated and measured values that vary greatly and randomly from each other. Factors not incorporated in Equation 1, such as permeability of the liquefied and overlying capping layer, may greatly affect lateral displacement in coarse grained materials. These factors render Equation 1 invalid for estimating displacements for liquefiable soils with $D50_{15}$ greater than 1 mm.

In addition to the specified limits on the values of F_{15} and $D50_{15}$ for which Equation 1 is valid, there are also limits on allowable combinations of these values. Fig. 13 shows a plot of F_{15} versus $D50_{15}$ for all of the data in the database compiled by Bartlett and Youd (1992). This plot shows a rather narrow band of combinations of F_{15} and $D50_{15}$ for which Equation 1 is valid. Extrapolation beyond these textural limits introduces uncertainty into the predicted displacements.

Further Restrictions on Use of Equation 1

Equation 1 was regressed from observed displacements at previous lateral spread sites. Most of those sites were located in areas underlain by broad deposits of liquefiable soil. In those few instances where data were collected from lateral spreads that traversed narrow or sinuous channels, displacements were generally much smaller than those predicted by Equation 1. For example, the lateral spreads that developed in the South of Market and Mission Creek zones of San Francisco during the 1906 earthquake moved only about 10% to 20% of the distance predicted by Equation 1. In those instances, nearby lateral boundaries apparently impeded displacement. (The nearness of the source, generally less than 12 km for a magnitude 7.9 earthquake, also adds to the uncertainty of these predicted values.) Similarly, near the edge (boundary) of a lateral spread, displacements are likely to be significantly reduced

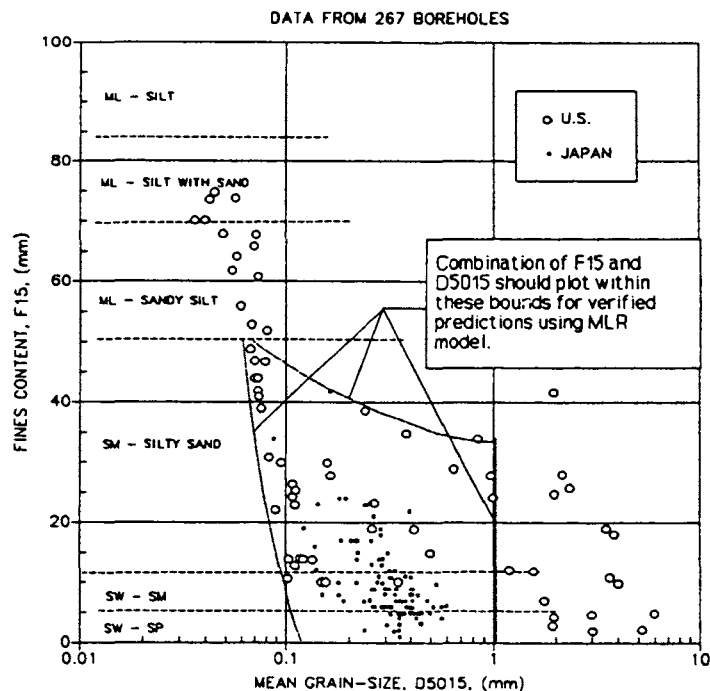


Fig. 13. Combinations of F_{15} and $D50_{15}$ From Lateral Spread Case History Data Base Compiled by Bartlett and Youd (1992)

by lateral boundary effects compared to displacements in the main body of the spread (see circled data on Fig. 8). Thus, Equation 1 may greatly over predict lateral displacements in narrow spread zones or near the boundaries of wider zones.

EXAMPLE CALCULATIONS

To illustrate the calculation of lateral ground displacement using Equation 1, consider the hypothetical soil stratigraphy and ground conditions shown on Fig. 14. Soil properties for the various layers are listed in Table IV and plotted on Fig. 12. This cross section depicts soil layers beneath a possible site for a large radar tower. The foundation for the tower is to be constructed with steel piles that could withstand up to 1.0 m of lateral displacement without impairment of their ability to support the radar tower. Thus, a primary design consideration is the magnitude of possible lateral spread displacements: will those displacements be less than or greater than 1 m at this site?

The design earthquake magnitude, source distance, and peak acceleration specified by engineering seismologists for this site are 6.5, 11 km, and 0.30 g, respectively. The site is a stiff soil site in the western U.S. The other parameters required for application of Equation 1 are determined as follows:

From the cross section of the site, the height of the free face (channel depth) is noted as 4.8 m. The planned tower is

located 45 m from the base of the free face. Thus, $W = (4.8 \text{ m}/45\text{m})(100) = 10.7\%$. The gentle ground slope of the terrain at the tower site is characterized by a rise of elevation of 0.3 m over a distance of 60 m yielding a ground slope, S , of 0.5%.

The soil stratigraphy and soil properties are noted in Fig. 12 and Table IV, respectively. From a review this information, and as noted in previous example calculations in this text, the liquefiable layer is divided into two sub-layers: Layer 1 is composed of sand to silty sand with a thickness, T_{15} , of 3.6 m, an average fines content, F_{15} , of 6.5%, and an average mean-grain size, $D50_{15}$, of 0.405 mm. Layer 2 is composed of silty sand with a T_{15} of 0.9 m, F_{15} of 43, and $D50_{15}$ of 0.11 mm. Application of those parametric values Equations 1a and 1b yields the following results:

(1) For free-face conditions:

For layer 1,

$$\begin{aligned} \text{Log } D_{H1} = & -16.366 + 1.1782 (6.5) - 0.9275 \text{Log}(11 \text{ km}) - \\ & 0.0133(11 \text{ km}) + 0.6572 \text{Log}(10.7\%) + 0.3483 \\ & \text{Log}(3.7 \text{ m}) + 4.527 \text{Log}(100 - 6.5\%) - 0.9224 \\ & (0.405 \text{ mm}) = -0.3972 \end{aligned}$$

$$\text{and, } D_{H1} = 0.40 \text{ m}$$

For layer 2,

$$\begin{aligned} \text{Log } D_{H2} = & -16.366 + 1.1782 (6.5) - 0.9275 \text{Log}(11 \text{ km}) - \\ & 0.0133(11 \text{ km}) + 0.6572 \text{Log}(10.7\%) + 0.3483 \\ & \text{Log}(0.9 \text{ m}) + 4.527 \text{Log}(100 - 43\%) - 0.9224 \\ & (0.11 \text{ mm}) = -1.3119 \end{aligned}$$

$$\text{and, } D_{H2} = 0.05 \text{ m}$$

The total free-face displacement is the sum of the component displacements:

$$D_H = 0.40 \text{ m} + 0.05 \text{ m} = 0.45 \text{ m}$$

(2) For ground slope conditions:

For Layer 1,

$$\begin{aligned} \text{Log } D_{H1} = & -15.787 + 1.1782 (6.5) - 0.9275 \text{Log}(11 \text{ km}) - \\ & 0.0133(11 \text{ km}) + 0.4293 \text{Log}(0.5\%) + 0.3483 \\ & \text{Log}(3.7 \text{ m}) + 4.527 \text{Log}(100 - 6.5\%) - 0.9224 \\ & (0.405 \text{ mm}) = -0.6239 \end{aligned}$$

$$\text{and, } D_{H1} = 0.24 \text{ m}$$

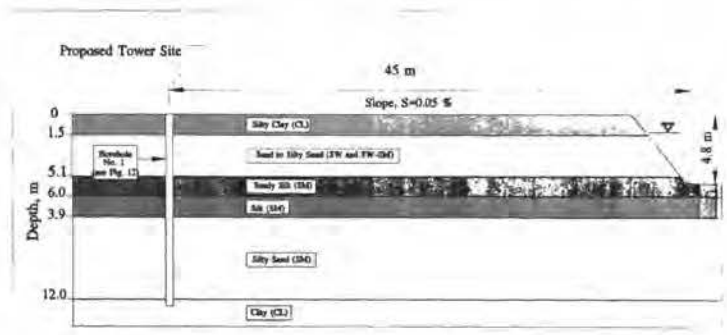


Fig. 14. Hypothetical Cross Section for Illustrative Radar Tower Site (After Youd, 1993)

For layer 2,

$$\begin{aligned} \text{Log } D_{H2} = & -15.787 + 1.1782 (6.5) - 0.9275 \text{Log}(11 \text{ km}) - \\ & 0.0133(11 \text{ km}) + 0.4293 \text{Log}(0.5\%) + 0.3483 \\ & \text{Log}(0.9 \text{ m}) + 4.527 \text{Log}(100 - 43\%) - 0.9224 \\ & (0.11 \text{ mm}) = -1.5387 \end{aligned}$$

$$\text{and, } D_{H2} = 0.03 \text{ m}$$

The total ground slope displacement is the sum of the component displacements:

$$D_H = 0.24 \text{ m} + 0.03 \text{ m} = 0.27 \text{ m}$$

Only the larger of the two estimated displacements need be used in the design analysis. In this instance, that displacement is 0.45 m. (If the designer wished to be ultraconservative, the displacements predicted for ground-slope conditions could be added to the free-face displacement. That degree of conservatism, however, is not required.)

The calculated displacement of 0.45 m is less than the allowable displacement of 1.0 m, indicating that the tower foundation is safe for the mean expected displacement. Because the tower supports an important radar scanning device, however, it may be classed as a critical structure, requiring a displacement with a high probability of not being exceeded. Based on Fig. 8, doubling of the displacement predicted by Equation 1 yields a value with a high probability of not being exceeded. In this instance the predicted displacement of 0.45 m should be doubled to 0.9 m for conservative design. This displacement, however, is only slightly less than the 1.0 m of allowable displacement. Thus, the structure is only marginally safe against liquefaction-induced lateral spreads that might possibly be generated by the design earthquake.

APPLICATIONS OF EMPIRICAL PROCEDURE

The empirical procedure developed by Bartlett and Youd (1992) is gaining wide use in geotechnical engineering practice. Displacement estimates have been developed for several sites for use as design considerations. For example, the author has consulted with a major electrical utility company concerning the safety of a transmission tower located in a liquefiable area near a river in a seismic area. The utility company had planned to move the tower at a cost in excess of \$1 million. Preliminary estimates indicate, however, that displacements at the site would not likely exceed the lateral deformation capacity of the timber piles supporting the tower. As a consequence, the planned expenditure to move the tower has been put on hold while additional borings and tests are conducted to better define stratigraphy and properties of sediments beneath the site. If the final analysis confirms or reduces the estimated displacement, a savings in the range of \$1 million will be realized by the company, without compromising the specified degree of safety required by company policy.

The British Columbia Gas Company recently evaluated the seismic safety of the gas transmission system in the lower mainland region. This evaluation was conducted by the company and EQE International, Inc., with the assistance of several consulting firms and private consultants including the author (EQE International, 1994). The empirical procedure of Bartlett and Youd was applied to estimate probable lateral spread displacements in liquefaction-prone areas. Many segments of pipeline, several gate stations, and a few other facilities were identified as vulnerable to damage due to lateral spreading. In particular, pipes adjacent to pipeline bends were identified as particularly vulnerable to liquefaction-induced damage. Pipeline bends tend to anchor these critical points and force greater flexural stresses into the adjacent pipes.

The Oregon Department of Geology and Mineral Industries (DOGAMI) recently published liquefaction hazard maps for the Portland Quadrangle, including a liquefaction susceptibility map with contours delineating thickness of liquefiable sediment beneath various parts of the quadrangle, and a lateral spread displacement map with contours delineating expectable lateral ground displacements (Youd and Jones, 1993; Jones et al., 1994). The latter map was compiled using the empirical technique of Bartlett and Youd (1992) to estimate displacements. Multiplication factors are listed in a table which may be used to correct displacements shown on the map for sediment textures and earthquake magnitudes different from those used as standards in calculating the contoured displacements.

The addition of probable ground displacement to liquefaction hazard maps, as was done for the Portland Quadrangle, allows the maps to be used for damage estimation, emergency planning, and preliminary engineering design.

SUMMARY

Ground failure is the primary cause of liquefaction induced damage during earthquakes. These failures may take several forms including flow failure, ground oscillation and lateral spread. Of these failure types, lateral spread is the most common and widespread. Lateral spreads usually develop on mild slopes or on flat ground near free faces, such as incised river channels, types of terrain where urban and industrial complexes are commonly developed. Many of these facilities have suffered severe damage due to lateral spread during past earthquakes.

Several analytical and empirical procedures have been proposed for estimating lateral spread displacement, including finite element models, elastic beam models, mechanistic sliding-block models, physical models, and empirical models. Of these, the mechanistic sliding-block model has been developed to a stage where design applications can be made by specialists, but more development and verification is required before the procedure can be routinely applied by non-specialists (Byrne and others, 1992).

An empirical model, regressed from a multiple linear analysis of case-history data, has been published by Bartlett and Youd (1992). This model has an advantage that site information and soil properties required in the analysis are those most commonly collected during routine site investigations. Procedures and example calculations are developed herein to guide geotechnical engineers and other specialists in properly applying this model for estimation of possible lateral spread displacements at liquefiable sites. Limitations to application of the model are also discussed. Further compilation of case history data and comparison with model performance will lead to needed additional verification and likely to model improvements.

REFERENCES

- Ambraseys, N.N. (1988), "Engineering Seismology," *Earthquake Engineering and Structural Dynamics*, (17)1:1-105.
- Bartlett, S.F., and Youd, T.L. (1992), "Empirical Analysis of Horizontal Ground Displacement Generated by Liquefaction-Induced Lateral Spread," *National Center for Earthquake Engineering Research, Technical Report NCEER-92-0021*.
- Byrne, P.M., Jitno, H., and Salgado, F. (1992), "Earthquake Induced Displacement of Soil-Structures Systems," *Proceedings, 10th World Conference on Earthquake Engineering, Madrid, Spain, 1407-1412*.

- EQE International (1994), "Seismic Risk Assessment of the BC Gas Transmission and Intermediate Pressure Natural Gas Pipeline System in the Lower Mainland Region," Unpublished report, EQE International, Inc. 18101 Von Karman Ave., Suite 400, Irvine, California.
- Finn, W.E.L., and Yogendrakumar, M. (1989), "TARA-3FL: Program for Analysis of Liquefaction Induced Flow Deformations," Department of Civil Engineering, University of British Columbia, Vancouver, B.C., Canada
- Hamada, M., Towhata, I., Yasuda, S., Isoyama, R. (1987), "Study of Permanent Ground Displacement Induced by Seismic Liquefaction," *Computers and Geotechnics*, Elsevier Applied Science Publishers, (4)4:197-220.
- Idriss, I.M. (1990), "Response of Soft Soil Sites During Earthquakes," *Proceedings, H. Bolton Seed Memorial Symposium*, BiTech Publishers, LTD, Vancouver, B.C. Canada, (2):273-290.
- Idriss, I.M. (in press), "Procedures for Selecting Earthquake Ground Motions at Rock Sites," A Report to the National Institute of Standards and Technology, U.S. Dept. of Commerce, Gaithersburg, Maryland.
- Jones, C.F., Youd, T.L., and Mabey, M.A. (1994), "Liquefaction Hazard Maps for the Portland, Oregon Quadrangle," *Proceedings, 5th National Conf. on Earthquake Engineering*, EERI, Chicago, IL. (4):209-218.
- Newmark, N.M. (1965), "Effects of Earthquakes on Dams and Embankments," *Geotechnique* (15)2:139-160.
- Prevost, J.H. (1981), "DYNA-FLOW: A Nonlinear Transient Finite Element Analysis Program," Report No. 81-SM-1, Department of Civil Engineering, Princeton University, Princeton, NJ.
- Seed, H.B., Tokimatsu, K., Harder, L.F., and Chung, R.F. (1985), "Influence of SPT Procedures in Soil Liquefaction Resistance Evaluations," *Journal of the Geotechnical Engineering Division, ASCE*, (111)12:1425-1445.
- Seed, R.B., Dickenson, S.E., Rau, G.A., White, R.K., and Mok, C.M. (1994), "Site Effects on Strong Shaking and Seismic Risk: Recent Developments and Their Impact on Seismic Design Codes and Practice," *Structural Congress II*, ASCE, (1):573-578.
- Towhata, I., Tokida, K., Tamari, Y., Matsumoto, H., and Yamada, K. (1991), "Prediction of Permanent Lateral Displacement of Liquefied Ground by Means of Variational Principle," *Proceedings, 3rd Japan-U.S. Workshop on Earthquake Resistant Design of Lifeline Facilities and Countermeasures for Soil Liquefaction*, National Center for Earthquake Engineering Research, Technical Report NCEER-91-0001:237-251.
- Yasuda, S., Nagase, H., Kiku, H., Uchida, Y. (1991), "A Simplified Procedure for the Analysis of the Permanent Ground Displacement," *Proceedings, 3rd Japan-U.S. Workshop on Earthquake Resistant Design of Lifeline Facilities and Countermeasures for Soil Liquefaction*, National Center for Earthquake Engineering Research, Technical Report NCEER-91-0001:25-236.
- Youd, T.L. (1993), "Liquefaction-Induced Lateral Spread Displacement," U.S. Navy, NCEL Technical Note N-1862.
- Youd, T.L., and Jones, C.F. (1993), "Liquefaction Hazard Maps for the Portland Quadrangle, Oregon," in *Earthquake Hazard Maps for the Portland Quadrangle, Multnomah and Washington Counties, Oregon, and Clark County, Washington, Oregon Department of Geology and Mineral Industries, Portland, Oregon, GMS-79: 1-1 to 1-17.*